



Effect of knurling shoulder design with polygonal pins on material flow and mechanical properties during friction stir welding of Al–Mg–Si alloy

Krishna Kishore MUGADA^{1,2}, Kumar ADEPU³

1. Department of Mechanical Engineering, Gayatri Vidya Parishad College of Engineering, Madhuwarada-530041, Vishakhapatnam, India;
2. Energy System Materials Lab, Department of Advanced Materials Engineering, Dong-Eui University, Busan 614-714, Korea;
3. Department of Mechanical Engineering, National Institute of Technology, Warangal-506004, Telangana, India

Received 29 December 2018; accepted 20 September 2019

Abstract: Understanding the material flow facilitated by tool geometry in friction stir welds is challenging for quality weld production in industrial applications. The optimal tool shoulder and pin design combination, which plays a vital role in material flow was addressed. The flow of plasticized material was analyzed using a marker insert technique. The results show that the knurling shoulder design with square and hexagonal pin design facilitated constant stability force with reference to weld length/time. The uniform mixing and distribution of plasticized material were facilitated by the knurling shoulder design with square tool pin shape ($(T_k)_s$ (sticking length minimum) below which fragmented copper was observed. ($T_k)_s$ tool facilitated higher mechanical properties for the welds, i.e. strength (182 MPa) and hardness (HV 78) in stir zone.

Key words: shoulder end feature; polygonal pins; material flow; axial force; mechanical properties

1 Introduction

Recent advances in the solid state joining processes, such as friction stir welding (FSW) have proved to be a greater advantage for joining of aluminum and its alloys, including 2xxx and 7xxx Al alloys [1]. The usage of FSW process by the industrial sector has been increased since it was patented by THOMAS and NICHOLAS [2]. FSW enables the joining of various combinations of similar–similar, similar–dissimilar metals namely Al–Cu, Al–Ti, and Al–SS, etc. [3].

The FSW process plasticizes and bonds the two workpieces in three stages: plunging, dwelling and traversing [4]. The FSW tool which interacts with the workpieces to be joined consists of a shoulder and pin. The shoulder generates more frictional heat and pin shears the surrounding material, and the plasticized material is transported to the trailing edge (TE) from the leading edge (LE) of the weld [5]. Typically, available shoulder geometries are plane, concave, and convex profiles for which extensive studies were carried

out [6–9].

During the welding/joining of 1 mm-thick sheets of copper, GALVAO et al [6] studied the influence of shoulder designs and observed that the shoulder designs generate more temperature, refine the grains, and improve the mechanical properties compared to flat and concave profiles.

CEDERQVIST et al [7] studied the joining of 5 mm-thick copper sheets using various shoulder end designs and noticed stable welds with convex tool geometry compared to concave and flat tool geometries. Further, SCIALPI et al [8] utilized various shoulder end designs in welding of Al 6082 alloy and noticed a significant change in the dimensions of the weld zone and heat input conditions with various shoulder profiles. The investigation of LEAL et al [9] on the scroll shoulder design revealed that the plasticized material was dragged into the channels of re-entrant features on the shoulder, shears in the channels and resulted in increased heat generation.

Few authors have investigated the influence of pin geometry on the weld formation, mechanical properties

and microstructure evolution [10–26].

ELANGO VAN et al [10,11] investigated the role of tool pin shape and noticed severe plastic deformation with non-circular pins compared to other pin shapes. BISWAS et al [12] varied the tool pin geometries and identified that the pin has a significant influence on the plastic deformation and less influence on heat generation. KHODAVERDIZADEH et al [13] performed butt welding of copper and observed that the square pin edges have the advantage of eccentricity which was useful for material shearing leading to grain refinement. Using taper cylindrical and various polygonal pins, IMAM et al [14] welded 6063 aluminum alloys and identified that welds with square pin shaped tool produced higher strength. MEHTA et al [15,16] explained the behavior of deformed material adhesion to the sides of the polygonal pins and found a relation for an optimum number of sides for a weld process condition. They observed that in higher weld pitch conditions, the pins with a smaller number of edges have no permanent adhesion. Moreover, pins with a greater number of sides experienced less stress compared to those with a smaller number of sides.

RAO et al [17] studied the effect of triangular and conical pin geometries and observed that the final weld zone shape depends on the tool geometry. AMIRAFSHAR and POURALIAKBAR [18] studied the influence of polygonal pins and noticed a drastic reduction of grain size in the weld zone. Further, they observed that superior properties were produced for welds with square pin shape compared to triangular or simple pin geometries.

YANG et al [19] studied the role of tool geometry and identified that the shoulder shape and pin shape were responsible for total heat generation. Further, they identified that the flat faces increase the temperature on the pin in the stir zone. SU and WU [20] numerically investigated the traverse force for various FSW tool pin profiles such as cylindrical, square, and triflute. They noticed that with an increase in the welding speed the traverse force increases and is high in the case of the cylindrical pin and low in the case of a triflute pin.

KHOJASTEHNESHAD et al [21] investigated the role of tool pin shape on the distribution of Al_2O_3 - TiB_2 reinforcement particles and identified that the particle distribution was more uniform with square and triangular pin profile compared to the other pin profiles. Similarly, PERIYASAMY et al [22] analyzed the effect of pin shapes and observed the maximum tensile strength for welds with square pin shaped tool. JAFARLOU et al [23] investigated the effects of pin geometry in friction stir welded Al 5086- Al_2O_3 nanocomposite and observed that the pulsating action of the square pin profile has resulted superior mechanical properties in the welds. MUGADA and ADEPU [24–26] studied the role of tool shoulder

profile and pin profiles and identified that each shoulder has a particular combination of a pin. In their study with the ridge shoulder it has an ideal combination with square pin profile compared to the other polygonal pins in terms of the uniform distribution of plasticized material. CHEN et al [27] studied the pin thread effect on material flow behavior using numerical simulation and identified the interfacial sticking inside the grooves of thread, and velocity zones alter the flow of plasticized material. On the influence of individual tool shoulder shapes and pin shapes, a considerable amount of research work has been carried out. However, the effect of the combined shoulder geometry and pin geometry on the flow of the deformed material and quality of the weld were limited. Therefore, in the present work, the knurling shoulder end feature design and their combined effect with various polygonal pins such as taper cylindrical, triangular, square, pentagon and hexagonal pins were studied. The investigation was extended to study pin geometry effects on material flow, axial force along the weld, macrostructure and mechanical properties of the welds during the friction stir welding of 6082 aluminum alloy.

2 Experimental

The workpiece and tool material were chosen as 6082 aluminum alloy (in T6 heat treated condition) and H13 tool steel, respectively. The aluminum alloy consists of 0.98% Mg, 1.15% Si, 0.52% Mn, 0.024% Cu, 0.046% Zn, 0.02% Cr, 0.0089% Ti and remaining 97.25% Al. The sheets of 280 mm × 70mm × 6 mm were prepared for friction stir welding in square butt joint configuration. H13 tool steel was identified as a suitable tool material for the welding of aluminum alloys from the previously published work [4].

Tool steel of grade H13 in as-received condition has a hardness of HRC 30–45. The as-received H13 tool steel was heat-treated as per the standards, which improves the hardness of H13 tool steel to approximately HRC55.

The knurling channels in FSW tools with various non-circular/circular pin shapes are shown in Fig. 1. The optimum parameters were selected based on the pilot experiments and the values are listed in Table 1. A numerically controlled 3T FSW machine (model: FSW-3T; make: RV machine tools, Coimbatore), was used for performing the experiments. For the force and torque measurements, the inbuilt data acquisition was utilized.

The overall material flow and deformation of the tool geometry were studied by the concept of the marker insert technique. Therefore, copper strips (which were of different colors and easily distinguishable) of 0.25 mm in

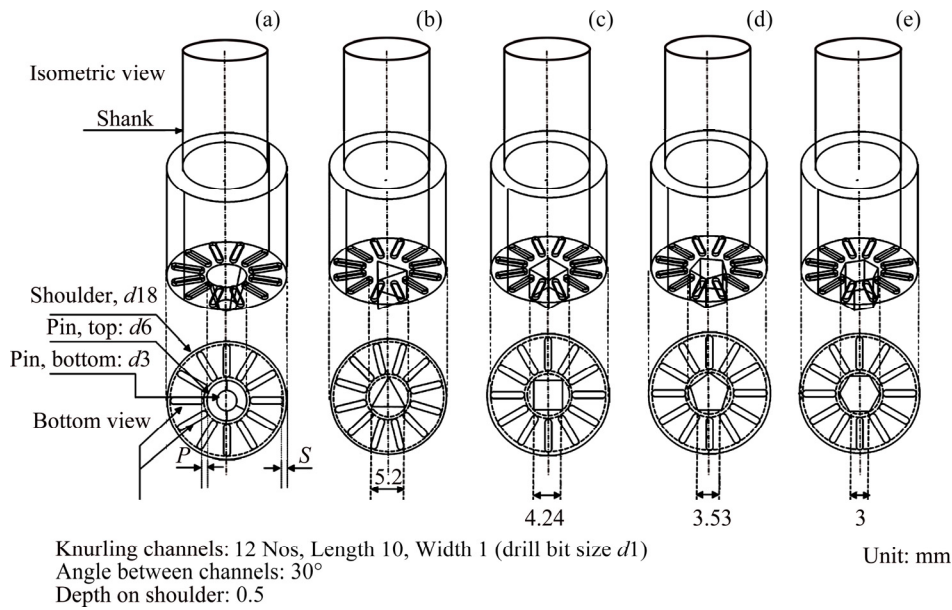


Fig. 1 Tools used during friction stir welding process showing knurling shoulder feature with taper cylindrical pin profile (T_K) (a), triangular pin profile ($(T_K)_T$) (b), square pin profile ($(T_K)_S$) (c), pentagonal pin profile ($(T_K)_P$) (d) and hexagonal pin profile ($(T_K)_H$) (e) (For all tools: Shoulder= d 18 mm; Pin= d 6 mm; Pin length=5.5 mm; $P=S$ =1, P and S are allowances from pin and shoulder, respectively)

Table 1 Optimum values of process parameters for defect-free weld condition

Process parameter	Value
Rotational speed of tool, $\omega/(r \cdot \text{min}^{-1})$	800
Traverse speed of tool, $V_f/(\text{mm} \cdot \text{min}^{-1})$	40
Tilt angle/ $^\circ$	1
Weld pitch for each cycle/ $(\text{mm} \cdot \text{r}^{-1})$	0.05
Tool plunge depth/mm	5.7

thickness were inserted at desired locations such as along/perpendicular to the weld direction/welding line as shown in Fig. 2. After welding, the samples were allowed to reach steady state condition, then sectioned samples were subjected to radiography and macroscopic studies (by milling off 3 mm from the top surface of welding) for studying the deformed/plasticized copper strips inside the weldments.

For tensile, hardness and metallographic studies, the weldments were cut perpendicularly to the weld direction.

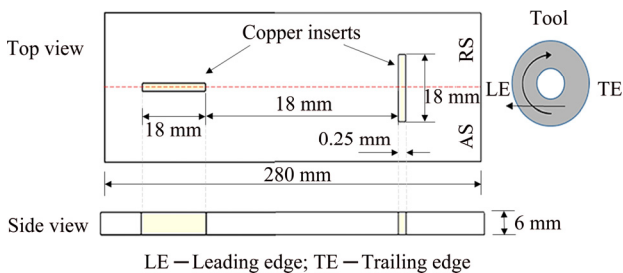


Fig. 2 Location of copper inserts in weld (Parallel to or along weld line (left) and perpendicular to weld line (right))

The cross-sections of the samples were roughly ground, polished with different emery paper grades (320–1000), cloth polishing and etched with modified poultants reagent (1 mL HF, 1.5 mL HCL, 2.5 mL HNO₃, and 95 mL distilled water). A 3D optical microscope (model: HRM 300; make: Huvitz, South Korea), was utilized to perform the macrostructural analysis of the metallographic samples. Along the mid-plane of the polished metallographic sample, the hardness was measured from advancing side to the retreating side of the weld at each 0.5 mm by using a Vickers hardness tester (model: ECONOMET; make: Chennai Metco Pvt Ltd, Chennai).

As per ASTM E8, the tensile samples were cut with the dimensions as shown in Fig. 3 using wire cut EDM

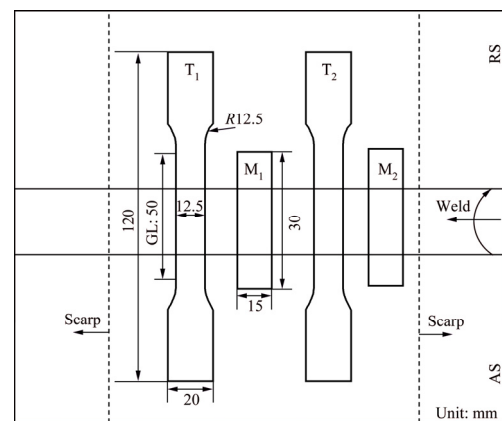


Fig. 3 Schematic layout of weldment showing various sample locations (Samples M_1 and M_2 were used for microhardness and metallography while T_1 and T_2 were used for tensile testing)

(electrical discharge machining). The tensile testing was performed at room temperature using a universal testing machine (UTM) (model: 300 LX, make: INSTRON) for evaluating the yield and ultimate tensile strength (UTS) of the weld sample.

3 Results and discussion

3.1 Tool axial force measurement

As shown in Fig. 4, during the plunging stage the sharp rise in the force occurs due to the initial resistance offered by the joining plates. The axial force for various non-circular pin profiles was almost equal to the taper cylindrical pin profile in the initial plunging phase.

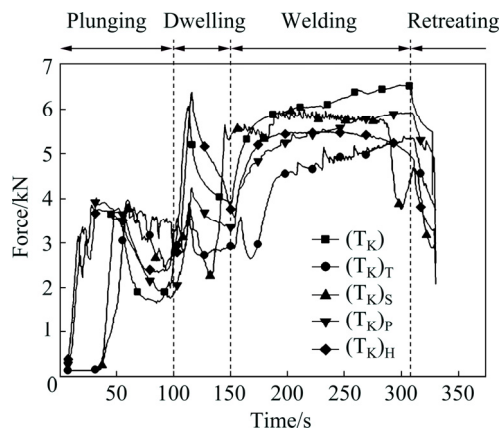


Fig. 4 Axial force plot during welding for various tools

At the start of dwelling stage, the shoulder readily touches the plates to be joined and raises the force to the maximum. This was because the shoulder contact area was more and more resistance was offered by the plates. As the dwelling continues, the material under the tool shoulder and around the tool pin plasticizes, therefore, softening of the material occurs, thereby force decreases. The knurling shoulder with hexagonal and taper cylindrical pins shows the maximum force during the dwelling. This can be attributed to the fact that for the hexagonal pin at six corners of pin the shearing occurs, therefore, the force required will be more followed by pentagonal, square, and triangle. However, the force required for the taper cylindrical pin profile was observed to be lower than the hexagonal pin because of the advantage of the taper angle and higher than the pentagonal pin because of the frictional contact condition.

At the start of welding, due to the sudden increment of tool traverse speed from 0 to 40 mm/min, a jerk of force was observed. Even though the same knurling shoulder was used during the experiments, a significant effect was observed in the force behavior with respect to the welding time by varying the pin profiles. The force required for taper cylindrical pin (T_R) was observed to be

higher and increasing with respect to time due to incompatibility flow generated by the tool (frictional action around the tool pin and shearing action under the tool shoulder).

An increasing behavior of force was observed during the welds produced with $(T_K)_T$ and $(T_K)_P$ tools over the weld time. This was attributed to more shearing volume produced by the odd faced edges of tool compared to the subsequent even number faced tool as explained by earlier researchers [15,16] and shown in Fig. 5. This was because the shearing at probe edge with odd instances causes the more sticking length due to the increased shear volume compared to the subsequent even instance pin, which increases the tool forces and leads to blunt edges of the odd faces at each weld cycle.

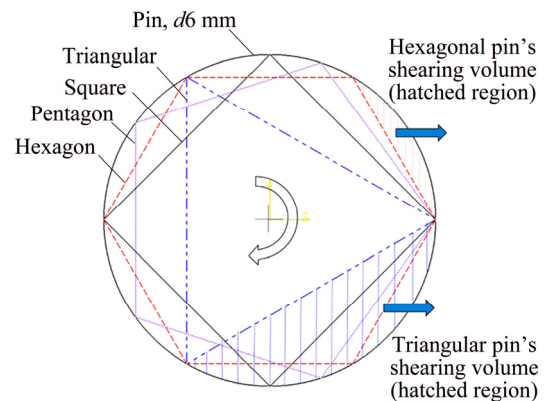


Fig. 5 Schematic sketch of shearing volume in dynamic condition for different non-circular pin shapes

For welds with $(T_K)_S$ and $(T_K)_H$, the force plot was observed to be almost uniform along the weld length due to the compatibility of pin and shoulder driven material flows (design constraint). For knurling shoulder design the additional plastic/shear deformation was better with square pin.

In general, the tools of flat shoulder geometry and the triangular shaped tool pin $(T_K)_T$ shear large amount of materials as shown in Fig. 5, resulting in increased forces [28]. Further, in the present work, it was observed that with the fixed shoulder end feature (knurling design) and by varying the pin geometry, higher forces were noticed for welds with even number faced (number of sides) pins such as square and hexagonal and lower forces for welds with odd faced pins during the welding time.

In an overview, the constant stability of force as noticed in $(T_K)_S$ and $(T_K)_H$ tool designs was more advantageous in the entire welding process.

3.2 Macrostructure of weld cross-section

Several regions were formed due to friction stir welding, as illustrated in Fig. 6, namely 1/1': heat

affected zone; 2/2': thermo-mechanically affected region; 3: weld nugget region.

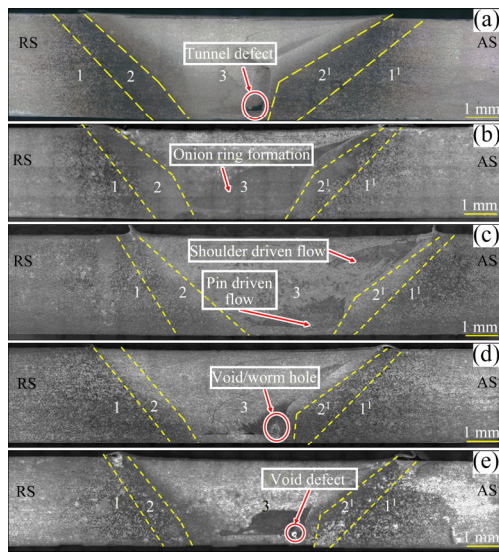


Fig. 6 Macrostructures of weld cross-section for welds with various tools (T_K) (a), (T_K)_T (b), (T_K)_S (c), (T_K)_P (d), and (T_K)_H (e)

Except in the welds with triangle and square tool pins, for all other welds, defects such as void/worm hole shown in Figs. 6(d) and (e) and tunnel defect shown in Fig. 6(a) were observed. This was because the combined influence of shoulder flow and pin flow was un-stable with non-uniform mixing and distribution of plasticized material as observed and explained in Section 3.3.

The width of darker band regions observed in Figs. 6(b–e) decreased from the triangular pin to the

hexagonal pin, and no such regions were observed in taper cylindrical profile. This was because the dynamic shearing volume of the triangular pin was more and as the number of sides increases, the volume of material sheared by the pin reduces. A weld line remnant was observed in all the welds and the line was found to be dragged towards the AS compared to the retreating side [29]. This was attributed to the basic nature of material flow which occurs from the retreating side to the advancing side.

3.3 Material flow

The flow of marker driven by shoulder (Fig. 7(a)) shows that the shoulder material dragged on retreating side (RS) was more compared to that on advancing side (AS) and Fig. 7(c) shows that the copper insert was deformed on AS/RS instead of mixing due to severe forces offered by the knurling shoulder. As observed in Fig. 7(b), the taper cylindrical pin, has deformed the material, not exceeding one pin diameter and a uniform flow spread region was observed to be more on RS compared to that on AS. In Fig. 7(d), as the weld advances, the material layers were dragged/deformed and pushed to RS over the weld length without mixing.

The deformed marker driven by the shoulder shown in Fig. 8(a) reveals the material dragged by the shoulder on the retreating side (RS) was less compared to the AS due to the cold and warm conditions of the workpiece material (basic flow nature). Figure 8(c) shows that the copper strip was dragged to AS, even though the shoulder design: knurling was constant for all the tool pins. Due to the large shear volume facilitated by triangular pin, the pin drives the shoulder material from

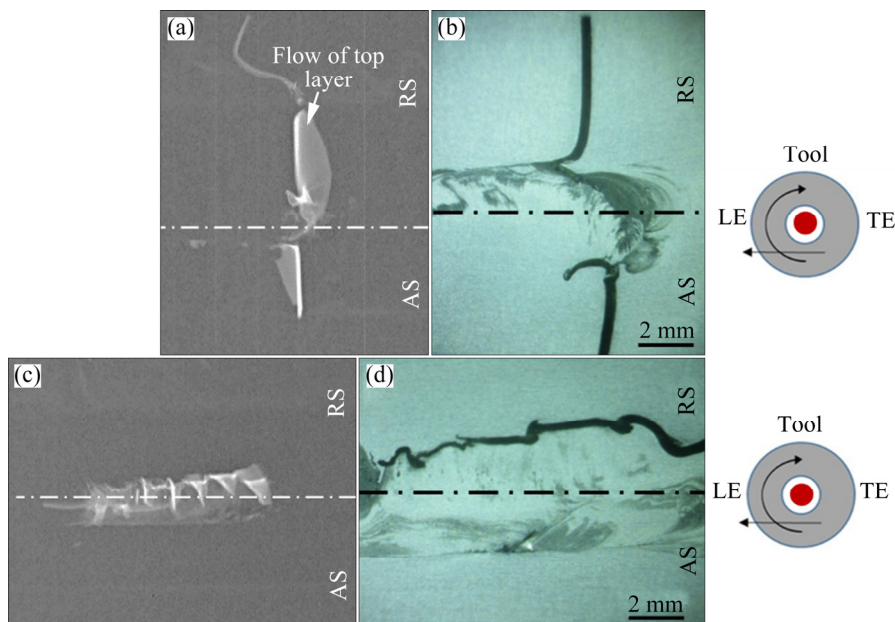


Fig. 7 Flow of deformed marker perpendicular (a, b) and parallel (c, d) to weld, radiography (left) and macrostructure (right) at 3 mm in depth from weld surface obtained with (T_K) tool

bottom to top and shoulder distributes the material on AS and RS.

As observed in Fig. 8(b), the triangular pin, has deformed and mixed the copper insert; however, few un-mixed fragments were observed on the AS due to the incompatible flow of shoulder and pin. The overall width of flow did not exceed the pin diameter and Fig. 8(d) showed layers of dragged material from RS towards AS and copper was spread on both AS and RS.

In Fig. 9(a) the deformed marker driven by shoulder shows that the material dragged on RS was more compared to that on AS due to knurling shoulder contact and Fig. 9(c) shows a partially mixed copper and thinning of initial copper size. As shown in Fig. 9(b), the complete mixing and distribution of fine copper

fragments on AS and RS around the tool pin by not exceeding one pin diameter (6 mm) were observed. This was because of high compatibility of shoulder-driven flow and pin-driven flow developed by knurling shoulder tool and square pin profile. Figure 9(d) shows a mixed flow region along the welding line due to the shearing action of the square pin profile.

Figure 10(a) shows that the shoulder drags more amount of material on RS compared to that on AS due to the initial contact and basic flow nature in FSW. Figure 10(c) shows fragments of copper pieces on AS and RS (un-mixed).

As observed in Fig. 10(b), fragmented and compressed copper insert was observed on AS due to the action of the pentagonal pin profile. Figure 10(d) shows

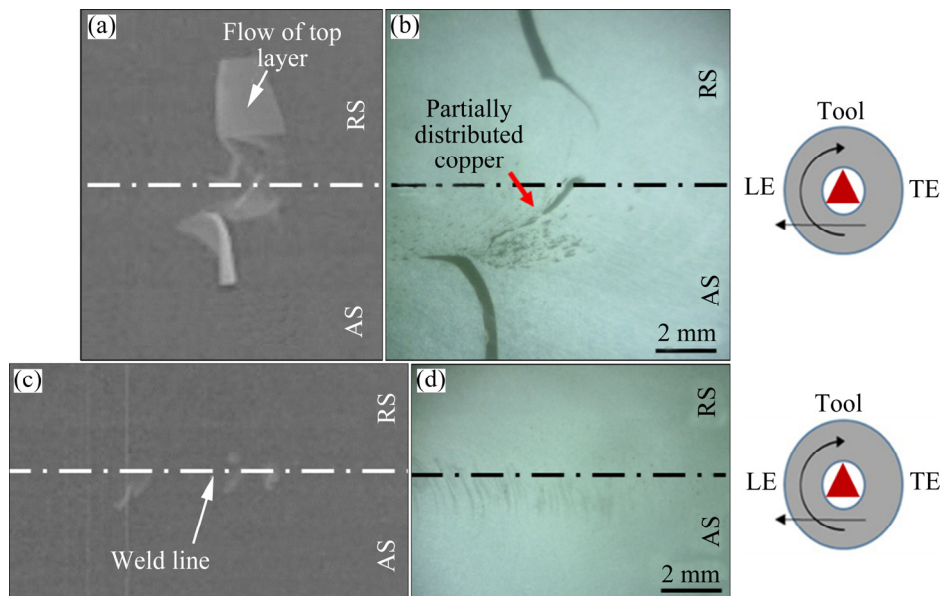


Fig. 8 Flow of deformed marker perpendicular (a, b) and parallel (c, d) to weld, radiography (left) and macrostructure (right) at 3 mm in depth from weld surface obtained with $(T_K)_T$ tool

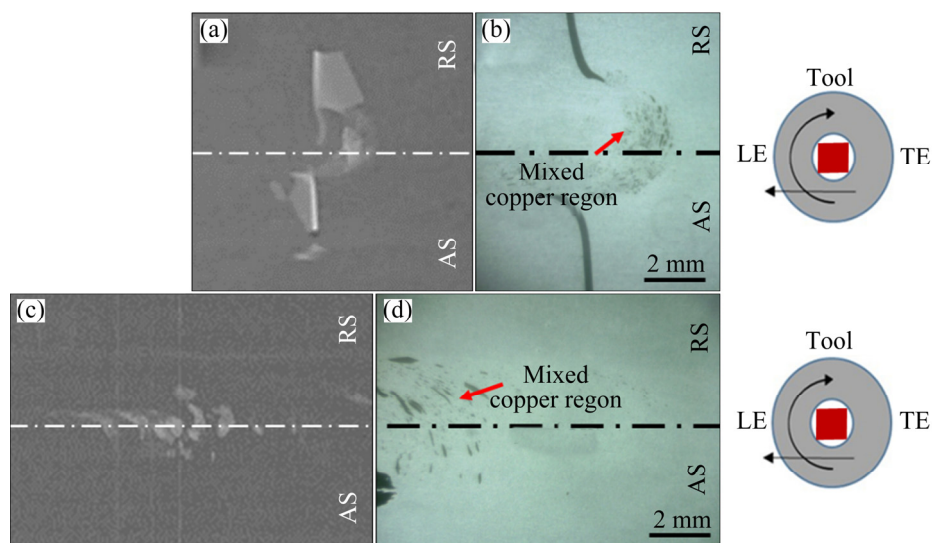


Fig. 9 Flow of deformed marker perpendicular (a, b) and parallel (c, d) to weld, radiography (left) and macrostructure (right) at 3 mm in depth from weld surface obtained with $(T_K)_S$ tool

that as the weld advances, the material layers were fragmented and distributed on AS and RS without complete mixing of material. This was due to the incompatibility of knurling shoulder with the pentagonal pin profile.

Figure 11(a) shows that a more thickness of the material was observed surrounding the pin and found decreasing on edge of the shoulder due to the effect of the thrust force by the pin on the top layers of the material. Figure 11(c) shows a fine layer of the un-mixed region in AS.

As observed in Fig. 11(b), the hexagonal pin and the flow of fragmented copper particles were deformed and distributed on both AS and RS. Figure 11(d) shows that a layer of material was dragged from RS and pushed towards AS.

3.4 Mechanical properties

The microhardnesses along the weld cross-section for different tools are shown in Fig. 12. It reveals that the tool pin design has considerable effects in the weld and heat affected regions.

As observed at the center, the hardness of welds with polygonal pins has more or less the same values and the lower hardness was observed in welds with triangular pins. This was due to the fact that the welds produced with a triangular pin, have more shearing volume and sticking length, which resulted in dynamic recrystallization of stir zone grains, which yields lower hardness. On the other hand, the welds with few polygonal pins have a distributed hardness around the plasticized volume of dynamic pin region (green color line) which was typically observed in the knurling

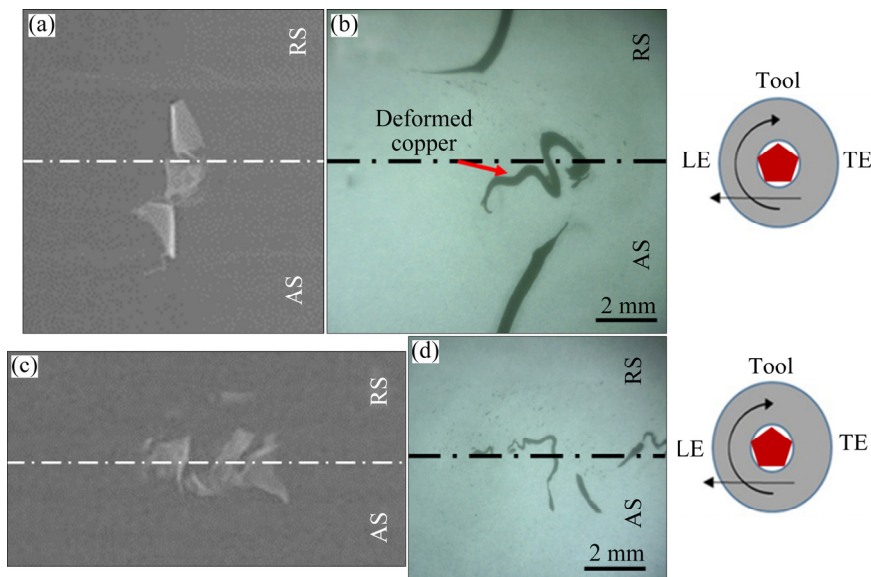


Fig. 10 Flow of deformed marker perpendicular (a, b) and parallel (c, d) to weld, radiography (left) and macrostructure (right) at 3 mm in depth from weld surface obtained with $(T_K)_P$ tool

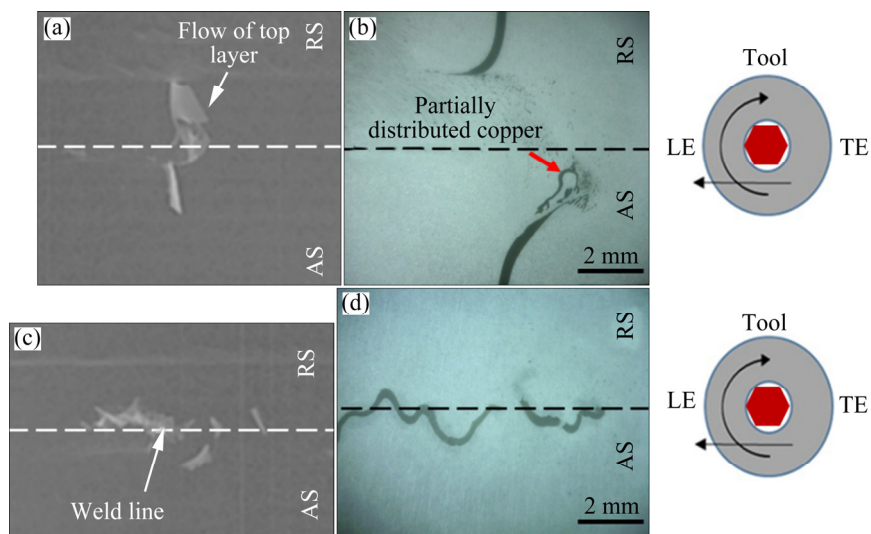


Fig. 11 Flow of deformed marker perpendicular (a, b) and parallel (c, d) to weld, radiography (left) and macrostructure (right) at 3 mm in depth from weld surface obtained with $(T_K)_H$ tool

Table 2 Force, torque and mechanical properties of welds with different tools

Sample No.	Tool	Number of sides (n)	Static to dynamic volume ratio	Axial force [#] /kN	Tool torque [#] /(kN·m)	UTS*/MPa	Avg. micro-hardness in stir zone* (HV)
1	Taper cylindrical pin shaped tool (T_K)		1	6.5	58.9	172±0.5	70.2
2	Triangular pin shaped tool (T_K) _T	3	2.4	5.4	48.5	178±1.0	62.1
3	Square pin shaped tool (T_K) _S	4	1.57	6.0	54.0	182±0.8	78.2
4	Pentagonal pin shaped tool (T_K) _P	5	1.32	5.9	53.1	171±0.6	80.6
5	Hexagonal pin shaped tool (T_K) _H	6	1.2	6.4	56.7	172±1.2	78.1

*Average of three reading values; # Maximum recorded force/torque in entire welding

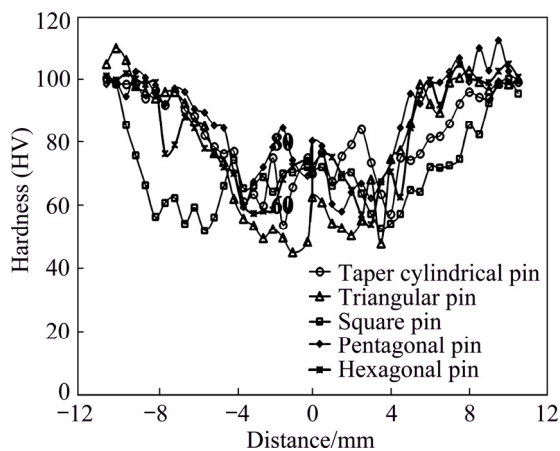


Fig. 12 Microhardness along mid plane of weld cross-section for welds with various tools

shoulder with square pin profile shape (with minimum sticking length).

Table 2 shows axial force for welds with polygonal pin tools, which shows the influence of pin, and is noticed to be increasing (in welding phase) with more number of flats/sides with a maximum for the hexagonal pin (6.4 kN) and minimum for the triangular pin (5.6 kN). The welds produced with a square pin tool produced superior mechanical properties, i.e., UTS of 182 MPa with a reasonable weld zone hardness HV 78.2.

4 Conclusions

(1) The force with reference to the weld time was almost constant during the welding with (T_K)_S and (T_K)_H tools due to the contact stability.

(2) The macrostructures revealed defects such as insufficient fusion, tunnel defects and void/worm hole, and in welds with (T_K) (T_K)_P, (T_K)_H tools because of the unstable flow caused by the combined shoulder and pin. Square pin with knurling re-entrant channels facilitated uniform distribution of plasticized material on retreating and advancing sides of weld.

(3) The darker pin influenced regions in the weld were observed to be high for triangular pin and low for the hexagonal pin, as the dynamic shearing volumes of the triangular and hexagonal pins were high and low, respectively.

(4) The welds fabricated with (T_K)_S tool were of superior properties with a UTS of about 182 MPa, and the weld nugget hardness was around HV 78 because of uniform mixing and distribution of plasticized material.

Acknowledgments

The authors thank the Mechanical Engineering Department, NIT Warangal, Telangana for providing the research facilities.

References

- [1] OLSON D L, SIEWERT T A, LIU S, EDWARDS G R. ASM handbook (volume 6): Welding, brazing, and soldering [M]. Materials Park, Cleveland, Ohio: ASM International, 2016.
- [2] THOMAS W M, NICHOLAS E D. Friction stir welding for the transportation industries [J]. Materials and Design, 1997, 18: 269–273.
- [3] NANDAN R, TARASANKAR D, BHADOSHIA H K D H. Recent advances in friction-stir welding—Process, weldment structure and properties [J]. Progress in Material Science, 2008, 53(6): 980–1023.
- [4] MISHRA R S, MOHANEY M W. Friction stir welding and processing [M]. Materials Park, Cleveland, Ohio: ASM International, 2007.
- [5] SCHMIDT H, JASPER H, JOHN W. An analytical model for the heat generation in friction stir welding [J]. Modelling and Simulation in Materials Science and Engineering, 2003, 12(1): 143–157.
- [6] GALVAO I, LEAL R M, RODRIGUES D M, LOUREIRO A. Influence of tool shoulder geometry on properties of friction stir welds in thin copper sheets [J]. Journal of Materials Process Technology, 2013, 213(2): 129–135.
- [7] CEDERQVIST L, SORENSEN C D, REYNOLDS A P, OBERG T. Improved process stability during friction stir welding of 5 cm thick copper canisters through shoulder geometry and parameter studies [J]. Science and Technology of Welding and Joining, 2009, 14(2): 178–184.
- [8] SCIALPI A, de FILIPPIS L A C, CAVELIERE P. Influence of shoulder geometry on microstructure and mechanical properties of friction stir welded 6082 aluminium alloy [J]. Materials and Design, 2007, 28(4): 1124–1129.
- [9] LEAL R M, LEITAO C, LOUREIRO A, RODRIGUES D M,

- VALICA P. Material flow in heterogeneous friction stir welding of thin aluminium sheets: Effect of shoulder geometry [J]. *Materials Science and Engineering A*, 2008, 498: 384–391.
- [10] ELANGO VAN K, BALASUBRAMANIAN V. Influences of tool pin profile and tool shoulder diameter on the formation of friction stir processing zone in AA6061 aluminium alloy [J]. *Materials and Design*, 2008, 29: 362–373.
- [11] ELANGO VAN K, BALASUBRAMANIAN V, VALLIAPPAN M. Effect of tool pin profile and tool rotational speed on mechanical properties of friction stir welded AA6061 aluminium alloy [J]. *Materials and Manufacturing Process*, 2008, 23: 251–260.
- [12] BISWAS P, A KUMAR D, MANDAL N R. Friction stir welding of aluminum alloy with varying tool geometry and process parameters [J]. *Proceedings of Institutions of Mechanical Engineering (Part B): Journal of Engineering Manufacture*, 2012, 226: 641–648.
- [13] KHODAVERDIZADEH H, HEIDARZADEH A, SAEID T. Effect of tool pin profile on microstructure and mechanical properties of friction stir welded pure copper joints [J]. *Materials and Design*, 2013, 45: 265–270.
- [14] IMAM M, BISWAS K, RACHERLA V. Effect of weld morphology on mechanical response and failure of friction stir welds in a naturally aged aluminium alloy [J]. *Materials and Design*, 2013, 44: 23–34.
- [15] MEHTA M, DE A, DEBROY T. Material adhesion and stresses on friction stir welding tool pins [J]. *Science and Technology of Welding and Joining*, 2014, 19: 534–540.
- [16] MEHTA M, REDDY G M, RAO A V, DE A. Numerical modeling of friction stir welding using the tools with polygonal pins [J]. *Defence Technology*, 2015, 11(3): 229–236.
- [17] RAO C V, REDDY G M, RAO K S. Microstructure and pitting corrosion resistance of AA2219 Al–Cu alloy friction stir welds—Effect of tool profile [J]. *Defence Technology*, 2015, 11(2):123–131.
- [18] AMIRAFSHAR A, POURALIAKBAR H. Effect of tool pin design on the microstructural evolutions and tribological characteristics of friction stir processed structural steel [J]. *Measurement*, 2015, 68: 111–116.
- [19] YANG M, BAO R J, LIU X Z, SONG C Q. Thermo-mechanical interaction between aluminum alloy and tools with different profiles during friction stir welding [J]. *Transactions of Nonferrous Metals Society of China*, 2019, 29(3): 495–506.
- [20] SU H, WU C. Determination of the traverse force in friction stir welding with different tool pin profiles [J]. *Science and Technology of Welding and Joining*, 2019, 24: 209–217.
- [21] KHOJASTEHEZHAD V M, HAMED H P, REZA V B. Effect of tool pin profile on the microstructure and mechanical properties of friction stir processed Al6061/Al₂O₃-TiB₂ surface hybrid composite layer [J]. *Proceedings of Institute of Mechanical Engineering (Part L): Journal of Materials and Design Applications*, 2019, 233: 900–912.
- [22] PERIYASAMY Y K, PERUMAL A V, BOOPATHIRAJA K P. Influence of tool shoulder concave angle and pin profile on mechanical properties and microstructural behaviour of friction stir welded AA7075-T651 and AA6061 dissimilar joint [J]. *Transactions of Indian Institute of Metals*, 2019, 72: 1087–1109.
- [23] JAFARLOU H, JAMALIAN H M, ESKANDAR M T. Investigation into the role of pin geometry on the corrosion behavior of multi-pass FSWed joints of Al5086 besides applying Al₂O₃ nanoparticles [J]. *Journal of Manufacturing Process*, 2018, 32: 425–431.
- [24] MUGADA K K, ADEPU K. Influence of ridges shoulder with polygonal pins on material flow and friction stir weld characteristics of 6082 aluminum alloy [J]. *Journal of Manufacturing Process*, 2018, 32: 625–634.
- [25] MUGADA K K, ADEPU K. Influence of tool shoulder end features on friction stir weld characteristics of Al–Mg–Si alloy [J]. *International Journal of Advanced Manufacturing Technology*, 2018, 99: 1553–1566.
- [26] MUGADA K K, ADEPU K. Role of tool shoulder end features on friction stir weld characteristics of 6082 aluminum alloy [J]. *Journal of Institution of Engineers Series C*, 2019, 100: 343–350.
- [27] CHEN G Q, LI H, WANG G Q, CUO Z Q, ZHANG S, DAI Q L, WANG X B, ZHANG G, SHI Q Y. Effects of pin thread on the in-process material flow behavior during friction stir welding: A computational fluid dynamics study [J]. *International Journal of Machine Tools and Manufacture*, 2018, 124: 12–21.
- [28] RAMANJANEYULU K, REDDY G M, RAO A V, MARKANDEYA R. Structure-property correlation of AA2014 friction stir welds: Role of tool pin profile [J]. *Journal of Materials Engineering Performance*, 2013, 22: 2224–2240.
- [29] JOLU T L, MORGENEYER T F, GOURGUES-LORENZON A F. Effect of joint line remnant on fatigue lifetime of friction stir welded Al–Cu–Li alloy [J]. *Science and Technology of Welding and Joining*, 2010, 15: 694–698.

搅拌针形状对 Al–Mg–Si 合金 搅拌摩擦焊过程中材料流动和力学性能的影响

Krishna Kishore MUGADA^{1,2}, Kumar ADEPU³

1. Department of Mechanical Engineering, Gayatri Vidya Parishad College of Engineering,
Madhuwarada-530041, Vishakhapatnam, India;

2. Energy System Materials Lab, Department of Advanced Materials Engineering,
Dong-Eui University, Busan 614-714, Korea;

3. Department of Mechanical Engineering, National Institute of Technology, Warangal-506004, Telangana, India

摘要: 了解搅拌摩擦焊中搅拌头几何形状对材料流动的影响对工业应用中的高质量焊接产品具有挑战性。讨论在材料流动中起重要作用的搅拌轴肩和搅拌针的最佳设计组合。采用标记插入技术对塑化材料的流动情况进行分析。结果表明,正方形和六边形的搅拌针滚花设计有利于与焊缝长度/时间相关的恒定力。正方形搅拌针(粘连长度最小)的轴肩滚花设计(T_K)_S有利于塑化材料均匀混合和分布,在搅拌针底部观察到了铜碎片。采用(T_K)_S 搅拌头的焊缝具有较高的力学性能,材料的搅拌区强度可达 182 MPa,硬度可达 HV 78。

关键词: 轴肩末端特征; 多边形搅拌针; 材料流动; 轴向力; 力学性能

(Edited by Xiang-qun LI)